

## Electroluminescence in Zinc Sulfide

W. A. THORNTON

*General Electric Research Laboratory, Schenectady, New York*

(Received October 6, 1955)

A simple theory, based upon a single-level trapping and field-controlled thermal release process, predicts detailed dependences of electroluminescence light output wave form and integrated light output on voltage, frequency, and temperature. Extensive data, obtained with the use of zinc sulfide phosphor powder layers, are in close agreement with the theory. Negligible frequency dependence of integrated light output at low fields and low temperatures and the usual strong dependence at higher fields are predicted and experimentally confirmed. Small temperature dependence, over a wide range of temperatures, at high fields and low frequencies, and strong dependence at lower fields, are predicted and observed; this explains the fact that both strong and weak temperature dependences are reported in the literature. Further correlations, together with the associated data, are presented.

### 1. INTRODUCTION

**E**LECTROLUMINESCENCE,<sup>1</sup> light emission resulting from the action of an electric field upon a phosphor crystal, apparently involves a number of competing and sequential electronic processes. The most common method of excitation of electroluminescence is by means of a sinusoidal voltage applied across a thin layer of phosphor; in this case these electronic processes combine in definite phase relationships to produce the characteristic periodic emission of visible light. The instantaneous light intensity is a complex function of time, consisting of a two-peak doublet per half-cycle in common electroluminescent phosphors. In general, the intensity of light emission is the only observable from which the nature and phase of the various electronic processes can be inferred. This paper presents a simple theory, based on electron trapping and field-controlled thermal release processes, of the major component of the characteristic light output wave form. Extensive experimental data which, together with much of that already published, are in close agreement with the theory are also presented.

Previous theoretical work<sup>1-4</sup> has dealt predominantly with mechanisms of excitation or ionization of the phosphor activator centers; when the light output wave form has been considered, prompt recombination and de-excitation has been assumed. However, Alfrey and Taylor<sup>5</sup> have had considerable success in explaining strong temperature dependence of light output by thermal release of trapped electrons.

Theory and experiment in this paper indicate that consideration of trapping and delayed processes is necessary to explain important experimental observations. Furthermore, much of published experimental data concern dependences of integrated light level on

applied rms voltage, frequency, and temperature. The importance of wave form analysis, rather than integrated light output, in leading to theoretical interpretation, is emphasized.

### 2. THE EXPERIMENTAL PHOSPHOR LAYER CELL

Uniform phosphor power layers clamped between plane electrodes, one of which is transparent, were utilized in the following experiments. No dielectric medium other than air at pressures between one atmosphere and  $10^{-5}$  mm Hg was used. Phosphor layer weights averaged  $2 \text{ mg/cm}^2$  and near 1 mil in thickness, corresponding to a phosphor-dielectric volume ratio of about 1:5. In a cell of this type, the electrodes are supported by phosphor aggregates in crystal-to-crystal electrical contact. The physical dispersion of the crystals is similar to that in conventional cells with plastic dielectric, since volume ratios are equivalent, yet electrical contact between the crystals (1) allows examination of conductive effects, (2) eliminates voltage division between phosphor and dielectric, (3) makes unimportant the correction for changes of dielectric constant of the medium with variables such as frequency and temperature. Light output wave forms are similar for powder-layer cells of the type described here, and for conventional plastic-dielectric cells. It is generally believed that field concentrations or barriers play an important part in electroluminescence, and that these can be described by a uniform volume density of positive charges in the phosphor crystal; in this case, the average field at low voltages will be proportional to  $\sqrt{V}$  and at higher voltages, when the electric field extends throughout the crystal volume, the average field will be proportional to applied voltage  $V$ . Dielectric strength in the air-dielectric cell is so great that, under the cell operating conditions of interest in this paper, breakdown does not occur.

### 3. LIGHT OUTPUT WAVE FORM: THEORY OF THE PRIMARY PEAK

The half-cycle doublets characteristic of electroluminescence with low-frequency sinusoidal voltage

<sup>1</sup> G. Destriau, *Phil. Mag.* **38**, 700 (1947).

<sup>2</sup> W. W. Piper and F. E. Williams, *Phys. Rev.* **87**, 151 (1952); *Brit. J. Appl. Phys., Suppl.* **4**, 39 (1954); *Phys. Rev.* **98**, 1809 (1955).

<sup>3</sup> D. Curie, *J. phys. radium* **14**, 510 (1953).

<sup>4</sup> Zalm, Diemer, and Klasens, *Philips Research Repts.* **10**, 205 (1955).

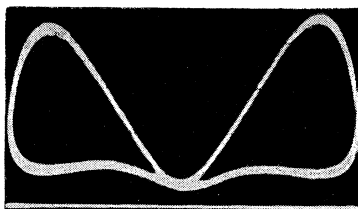
<sup>5</sup> G. F. Alfrey and J. B. Taylor, *Brit. J. Appl. Phys., Suppl.* **4**, 44 (1954); *Proc. Phys. Soc. (London)* **68**, 775 (1955).

excitation can be analyzed into two components of approximately Gaussian shape in time; the leading, or earlier, component is always larger in integrated area and is termed the primary peak, while the smaller component is termed the secondary peak.<sup>6</sup> The position in phase of these components is basic to theoretical analysis. A graphic indication of the phase relationships of the light components to the impressed voltage wave is obtained by applying the sinusoidal voltage to the X-plates of an oscilloscope and the light signal to the Y-plates. Figure 1 is a photograph of the repetitive oscilloscope trace, showing the zero-light baseline, with  $V=0$  at the center and  $V_{\max}$  at the extremities. The X-axis is then linear with instantaneous applied voltage and the Y-axis is linear with instantaneous light intensity, the light signal being obtained from a multiplier phototube and cathode follower circuit. It is apparent that the light components straddle the voltage maximum, the primary peak leading and the secondary peak lagging, and both components are out of phase but by considerably less than 90 degrees.

The following theory of the primary light peak is a close analogy to the classic thermal glow curve theory.<sup>7</sup> Assume that the initial state, at  $V=0$ , is similar to that of the thermal glow curve; that is, in the phosphor crystal there are  $N_0$  ionized activator centers and a supply of trapped electrons or donor levels. The light output level  $L$ , proportional to the recombination rate  $dN/dt$ , is proportional to the product of number  $N$  of ionized activator centers remaining at time  $t$  and the time rate of release of electrons from the trapping or donor (coactivator) levels. Experiment shows that the volume density of activators emitting light per half-cycle is no greater than  $10^{14}$  cm<sup>-3</sup>, while the volume density of coactivators is nearer  $10^{18}$  cm<sup>-3</sup>. Therefore  $dN/dt \propto Np$ , where  $p$  is the release probability of a trapped electron, given by  $p = s \exp(-E_0/kT)$ . Here, as usual,  $s$  is the frequency factor,  $E_0$  the trap depth in electron volts,  $k$  Boltzmann's constant, and  $T$  the absolute temperature.

In the presence of an electric field, the effective trap depth will decrease and more rapid field-controlled thermal release of electrons will occur; because of the periodicity of the trapping sites, the decrease in trap depth will be proportional<sup>8</sup> to the field rather than to

FIG. 1. Experimental light-output wave form; 60 cps, 50 volts rms, room temperature. Light increasing upward, instantaneous voltage zero at center, maximum at left and right.



<sup>6</sup> Zalm, Diemer, and Klasens, Philips Research Repts. 9, 8 (1954).

<sup>7</sup> J. T. Randall and M. H. F. Wilkins, Proc. Roy. Soc. (London) A184, 999, 347 (1945).

<sup>8</sup> N. F. Mott and R. W. Gurney, *Electronic Processes in Ionic Crystals* (Oxford University Press, Oxford, 1948), p. 42.

the half-power of the field as in the case of an isolated Coulomb potential. Assuming that the average field is proportional to the applied potential difference  $V = V_0 \sin \omega t \equiv V_0 \sin x$ , one obtains

$$\begin{aligned} \frac{dN}{dt} &= -Np \\ &= -Ns \exp \left[ - \left( E_0 - e \frac{a_0}{l} V_0 \sin \omega t \right) / kT \right], \end{aligned}$$

where  $e$  is the electronic charge,  $a_0$  the trap half-width, and  $l$  the extent of the electric field. When  $N$  is eliminated, the instantaneous light output is given by

$$L \propto N_0 e^{-E_0/kT} e^{a \sin x} \exp \left( -b \int e^{a \sin x} dx \right), \quad (1)$$

where  $a = (ea_0/l)(V_0/kT)$ ,  $b = (s/\omega)e^{-E_0/kT}$ , and  $x = \omega t$ . This function has the shape characteristic of a conventional thermal glow curve, rising slowly to a peak, from a value greater than zero, followed by a more rapid decrease toward zero. The quantity  $N_0$  may be a function of temperature, frequency, and voltage. The second exponential factor behaves like the release probability  $p$ , increasing with voltage or time from unity at  $V=0$ . The last exponential factor is proportional to the number  $N$  of ionized activators remaining at time  $t$ .

Of the  $10^{18}$  coactivator sites per cubic centimeter, about  $10^{16}$  cm<sup>-3</sup> are thermally ionized at room temperature and govern the distribution of electric field. Therefore the maximum density,  $10^{14}$  cm<sup>-3</sup>, of ionized activator centers has little effect on the field distribution, nor does the associated fluctuation of  $10^{14}$  cm<sup>-3</sup> in density of donor (coactivator) electrons show up

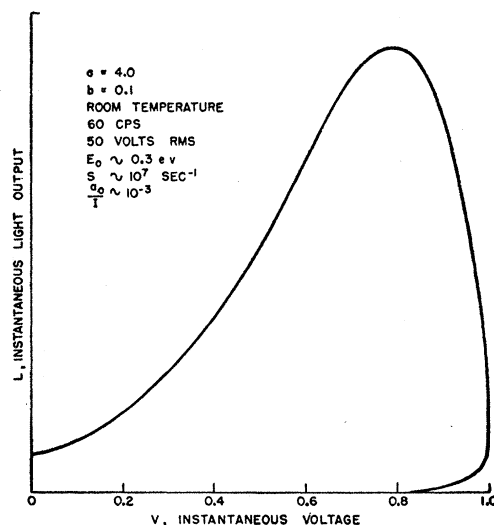


FIG. 2. Theoretical light-output wave form for the primary peak, at 60 cps, 50 volts rms, room temperature, for comparison to the experimental trace of Fig. 1.

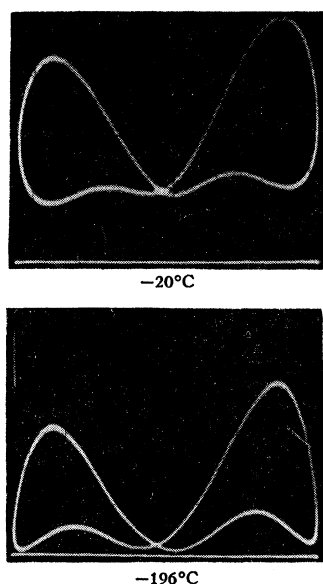


FIG. 3. Oscilloscope traces illustrating the temperature dependence of light output at  $V=0$ .  $F=60$  cps;  $V=50$  volts rms.

against the average density of  $10^{18}$   $\text{cm}^{-3}$ ; this average donor density is replenished at each ionization process.

#### 4. CORRELATION TO EXPERIMENT

Equation (1) can be fitted by adjustment of parameters  $a$  and  $b$  to the primary peak wave form of a conventional green-emitting, copper-activated electroluminescent phosphor at room temperature, 60 cps and 50 volts rms, for instance; this requires approximate values of  $a=4.0$  and  $b=0.1$ , corresponding to a single trap depth at 0.3 eV, frequency factor near  $10^7$   $\text{sec}^{-1}$ , and trap dimension something like 200 Å. The fit is shown in Fig. 2, where the theoretical wave form to be compared to the experimental oscilloscope trace appears.

Variations of both the shape of the wave form and of integrated light output  $L_I$  with peak voltage, frequency,

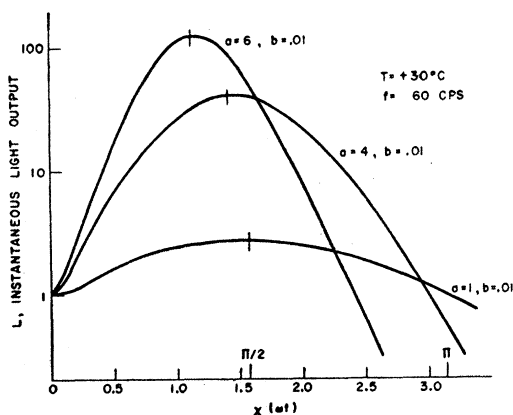


FIG. 4. Theoretical peak shift toward earlier times with increase in peak voltage  $V_0$ .

and temperature may be obtained from Eq. (1) by varying parameters  $a$  and  $b$  in the time-dependent exponential factors, and  $T$  in the first exponential. First, however, light emission at  $V=0$  is considered.

#### (a) Light Level at $V=0$

The important zero-voltage light level dependence upon temperature should be emphasized. At  $V=0$  and  $t=0$ , Eq. (1) gives

$$L_0 \propto N_0 e^{-E_0/kT}.$$

This means that the light output should be greater than zero even at the zeros of the voltage cycle, and the intensity at these points should be strongly temperature-dependent. Experimentally, the light output at  $V=0$  and room temperature is large, amounting to as much as 50% of peak intensity in some cases. This light level is observed to decrease rapidly with temperature decrease, evidently approaching zero; this decrease is illustrated by the traces of Fig. 3. Such behavior is, of course, easily explained by the trapping effects considered in this paper, and lends strong support to the theory. Whether the light level at  $V=0$  at liquid nitrogen temperature is actually many orders of magnitude less than that at  $20^\circ\text{C}$  is experimentally indeterminate, both because of overlap of the primary and secondary components at  $V=0$ , and because detecting such a low level in the presence of strong emission during other parts of the voltage wave is a difficult signal-to-noise problem.

At constant temperature,  $L_0 \propto N_0$ , where  $L_0$  has been arbitrarily defined as the light intensity at the minima of the observed wave form. Experimentally,  $N_0 \propto \exp(-C/V_0)$ , where  $C$  is a constant, at higher voltages where  $L_0$  is large enough for accurate measurement; the data cover four decades of light level. Also,  $N_0 \propto \sqrt{f}$  over a four-decade experimental variation of frequency  $f$ .

#### (b) Wave Form vs Peak Voltage

Increase in peak voltage corresponds to an increase in parameter  $a$ . The factor  $e^{a \sin x}$  in expression (1) behaves like the release probability  $p$ , increasing with voltage from an initial low value. As peak voltage  $V_0$  is increased,  $e^{a \sin x}$  is larger at a given point in the cycle and will lead to an earlier peaking of the instantaneous light output  $L$ . The theoretical peak shift with voltage increase is shown in Fig. 4. Agreement is evident in the series of photographs of Fig. 5. This peak shift with voltage was first observed experimentally by Destriau.<sup>1</sup>

#### (c) Wave Form vs Frequency

As angular frequency  $\omega$  is increased, corresponding to a proportional decrease in parameter  $b$ , the last exponential factor, describing depletion of ionized activators, becomes less significant. The wave-form peak

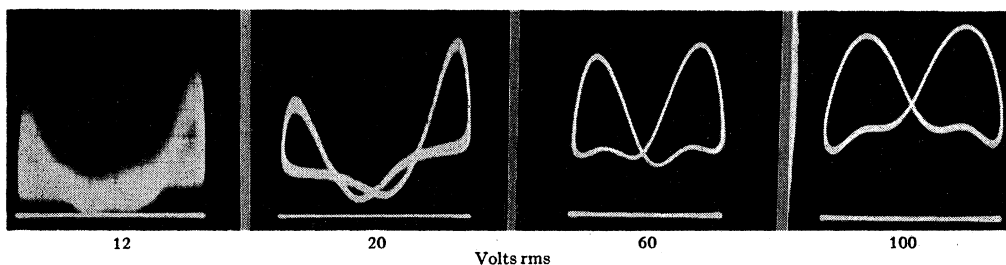


FIG. 5. Experimental wave forms showing the peak shift toward earlier times with increase in peak voltage  $V_0$ .  $F=60$  cps;  $T=+30^\circ\text{C}$ .

moves toward later times, until this factor becomes constant and the wave form takes on the shape of the function  $e^{a \sin x}$ . This shift is shown by the theoretical curves of Fig. 6 and experimental agreement by the oscilloscope traces of Fig. 7. The presence of the secondary peak is a complicating factor at high frequencies; nevertheless, the symmetry corresponding to the  $e^{a \sin x}$  function is evident.

#### (d) Wave Form vs Temperature

Decrease in temperature is equivalent in expression (1) to an increase in effective trap depth. Decrease in temperature should therefore lead to later onset of depletion and a shift of the peak toward later times. This shift is shown by the theoretical curves of Fig. 8; it is observed experimentally over much of the temperature range as shown by the photographs of Fig. 9. The small anomalous shift at very low temperatures is accounted for by the observations that (1) a strong blue component is added to the green emission, in the neighborhood of  $-200^\circ\text{C}$ , in both photoluminescence and electroluminescence, and that (2) this blue emission does peak considerably earlier in the voltage cycle, than the green light, as shown by wave-form detection through a spectrometer.

#### (e) Integrated Light Output $L_I$ vs Peak Voltage

Light output per cycle, per unit number of ionized activators at  $V=0$ , must increase with voltage and then level off as complete depletion of these activators during the cycle occurs. Graphical integration of the time-dependent exponential factors of Eq. (1), to obtain their contribution to the integrated light output, shows the expected behavior which also follows the relation  $\exp(-C/E)$  to a close approximation, the same form observed for  $N_0$ . Therefore, Eq. (1) may be rewritten to give the field dependence of  $L_I$  as

$$L_I \propto e^{-(C_1+C_2)/E},$$

where  $C_1$  is related to  $N_0$  and the ionization process, and  $C_2$  is related to the time-dependent factors of Eq. (1). In Fig. 10 appear data for  $L_I$  plotted against  $V_0^{-1}$ , valid at lower voltages, and in Fig. 11 plotted against  $V_0^{-1}$ , valid at higher voltages; it is evident

that  $V_0^{-1}$  is a fair description over the entire voltage range, while  $V_0^{-1}$  is poor at low voltages but gives a better fit at higher voltages, above 30 volts.

#### (f) Integrated Light Output $L_I$ vs Frequency and Temperature

In order to avoid color shift, with frequency and temperature, associated with the presence of both blue and green emission bands in the ZnS:Cu, Al, a phosphor containing additional manganese and showing only a single emission band in the yellow was used to obtain the data in this section.

In deriving Eq. (1), the expression

$$N = N_0 \exp\left(-b \int e^{a \sin x} dx\right)$$

is obtained, where  $N$  is the number of ionized activators remaining at point  $x$  of the cycle. The light output per

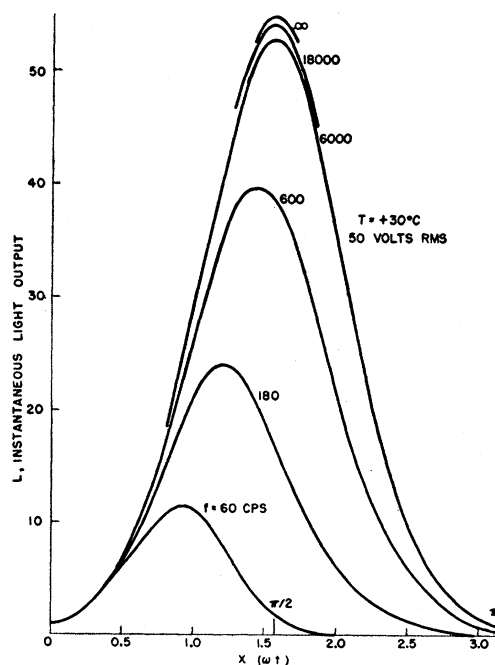


FIG. 6. Theoretical wave forms with variation in frequency plotted against time.

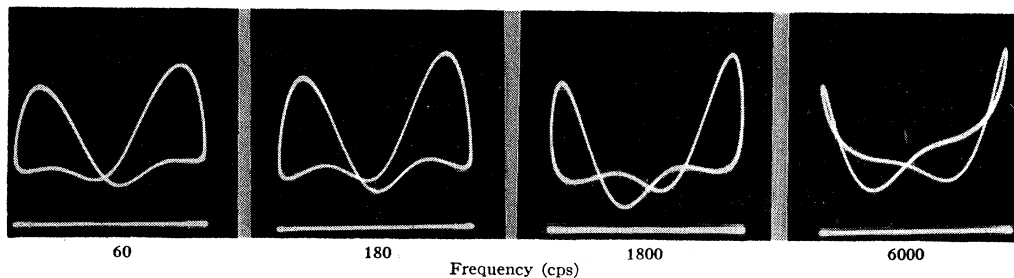


FIG. 7. Experimental wave forms with variation in frequency.  $T=30^{\circ}\text{C}$ ,  $V=50$  volts rms.

cycle from the primary peak is assumed proportional to the depletion of ionized activators and therefore to  $(N_0 - N_{2\pi})$  or to

$$1 - \exp\left(-b \int_0^{2\pi} e^{a \sin x} dx\right).$$

This quantity multiplied by the frequency yields the theoretical curves for integrated light output *vs* frequency of Fig. 12, for a "high" voltage (50 volts rms,  $a=4.0$ ) and a "low" voltage (12 volts rms,  $a=1.0$ ). Also plotted are data taken at the two voltages and fitted to the theoretical curves at one point. At very low voltages, depletion of the ionized activators does not occur during the cycle even at lower frequencies, and  $N_0$  is expected to be independent of frequency. Therefore agreement between theory and experiment should be and is observed. The frequency dependence of  $L_I$  at low voltages becomes very small. At high voltages, however, depletion of ionized activators is

strong and, as mentioned previously,  $n_0$  varies experimentally as  $f^3$ ; this is related to the observation that integrated light output *vs* frequency approaches a slope of  $\frac{1}{2}$  at high frequencies, rather than a slope of zero as integration of the time dependent factors predicts. The over-all frequency dependence of  $L_I$  at high voltages is strong.

The temperature dependence of integrated light output  $L_I$  depends upon the three exponential factors of Eq. (1). Graphical integration of these factors yields the theoretical curves of integrated light output *vs* temperature of Fig. 13, for a "high" voltage (100 volts rms,  $a=8.0$ ) and a "low" voltage (12 volts rms,  $a=1.0$ ). The general characteristics of the curve, for both voltage ranges, appear not to change, the curve merely shifting toward lower temperatures with increase in voltage. The rapid rise, of light output, from low temperatures followed by a leveling off at higher temperatures was first observed experimentally by Destriau.<sup>1</sup> Within an extended temperature range, not including very low temperatures, the theory predicts strong temperature dependence of integrated light output at low voltages and small temperature dependence at very high voltages. Support is seen in the experimental curves which show a much stronger temperature dependence at 15 volts than at 50 volts. An increase in voltage is theoretically equivalent to a decrease in frequency since depletion of ionized activators during the cycle is more severe; temperature dependence is therefore minimized at high voltage and low frequency. The data of Roberts<sup>9</sup> taken at a high voltage (150 volts rms; thickness  $\sim 5$  mils) over a limited temperature range, show only weak temperature dependence, while those of Alfrey and Taylor<sup>5</sup> on large single crystals (low average fields) show strong temperature dependence. Where integrated light output levels off<sup>5</sup> at very low temperatures, or shows an increase,<sup>10</sup> an additional process must be called upon to explain the data. The present theory is consistent with what is generally observed, small temperature dependence at high applied fields, and decreasing light output with decreasing temperature at low fields.

Another way of illustrating the interdependences of

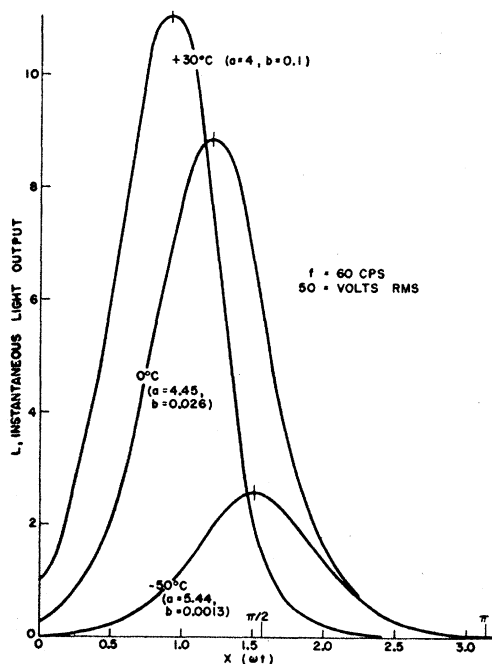


FIG. 8. Theoretical wave forms with variation in temperature.

<sup>9</sup> S. Roberts, J. Opt. Soc. Am. 42, 850 (1952).

<sup>10</sup> P. D. Johnson and F. E. Williams (to be published).

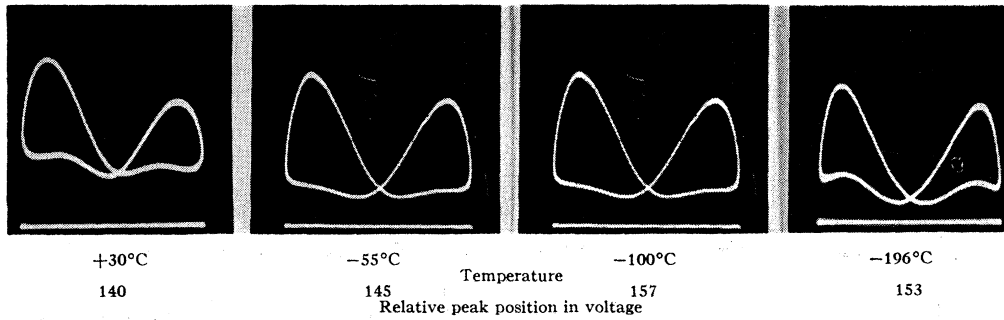


FIG. 9. Experimental wave forms with variation in temperature.  $F = 60$  cps;  $V = 50$  volts rms.

integrated light output  $L_I$  among voltage, frequency, and temperature is by means of the four experimental curves of Fig. 14. It is important to note that these extrapolated curves intersect in pairs at voltage extremes. Although these intersections may be poorly defined if complete families of curves are considered, the following important trends are apparent: (1) Frequency dependence of  $L_I$  is a maximum at high fields and high temperatures, and minimum at low fields and low temperatures. This is accounted for by the theory simply by the absence of depletion of ionized activators under the latter conditions. That is, with low fields and low temperatures, the last exponential factor in Eq. (1) never differs appreciably from unity; then the light output per cycle depends only upon the time per cycle, and  $L_I$  is frequency-independent. (2) Temperature dependence of  $L_I$  is a maximum at low fields and high frequencies, and minimum at high fields and low frequencies. Here, no temperature dependence is ex-

pected under conditions of extreme depletion, for all of the ionized activators recombine each cycle regardless of the temperature dependence of the release rate.

Commercial electroluminescent cells, often run at low frequencies and high voltages (60 cps and near breakdown voltages), should show little temperature dependence and strong frequency dependence of integrated light output. Temperature dependence in single crystals should vary as the number of barrier regions in the crystal; multiple barriers plus relatively large dimensions would be expected to show the strong temperature dependence characteristic of low average fields.

#### (g) Trapping Levels by Conventional Glow Curve

Finally, conventional glow curves were run on the ZnS phosphor cells used in obtaining the experimental data in this paper. The cells were cooled to liquid nitrogen temperature, irradiated with 3650 Å ultra-

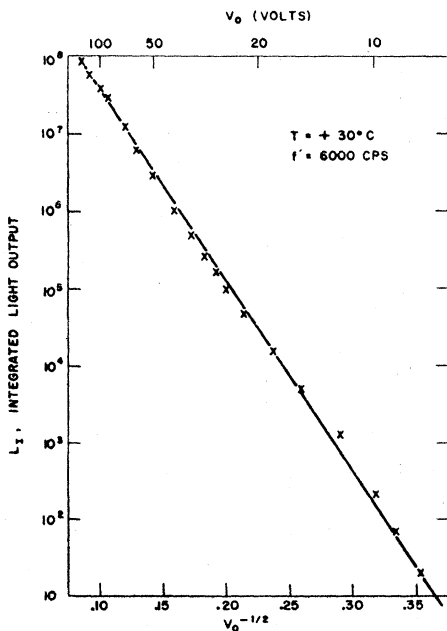


FIG. 10. Integrated light output  $L_I$  vs peak voltage  $V_0^{-1/2}$ , valid at lower voltages.

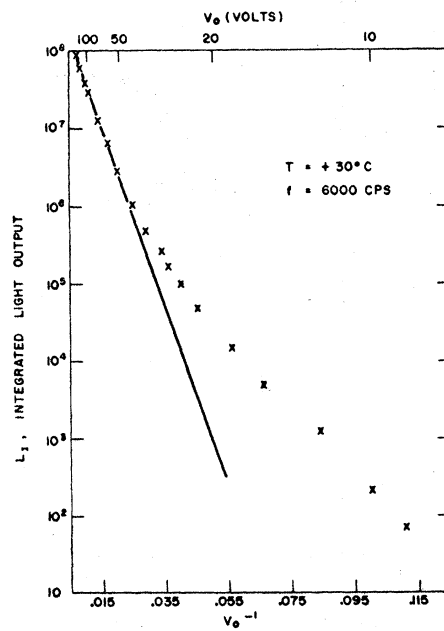


FIG. 11. Integrated light output  $L_I$  vs peak voltage  $V_0^{-1}$ , valid at higher voltages.

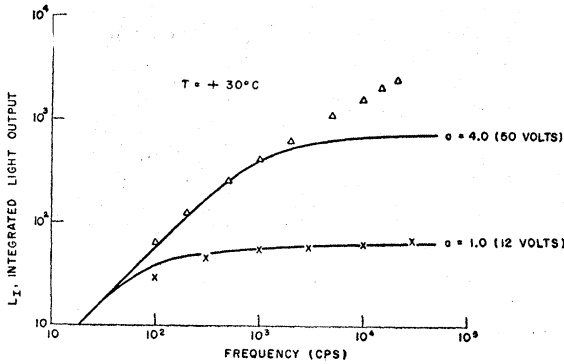


FIG. 12. Integrated light output  $L_I$  vs frequency  $f$ . Solid curves theoretical, plotted points experimental; curves fitted at one point.

violet light, the light source removed, and light emission as a function of temperature obtained during gradual warming of the cell. The resulting glow curves appear in Fig. 15 and indicate trapping levels in the range 0.2–0.3 ev. A level near 0.3 ev is found in many types of ZnS phosphors,<sup>11</sup> including copper-activated<sup>12</sup> and manganese-activated<sup>13</sup> zinc sulfides of the type used here. As the deeper traps will fill first and empty last, they will have the greater effect on the primary peak as regards peak shifts and peak heights. The net effects should closely approximate the theoretical dependencies

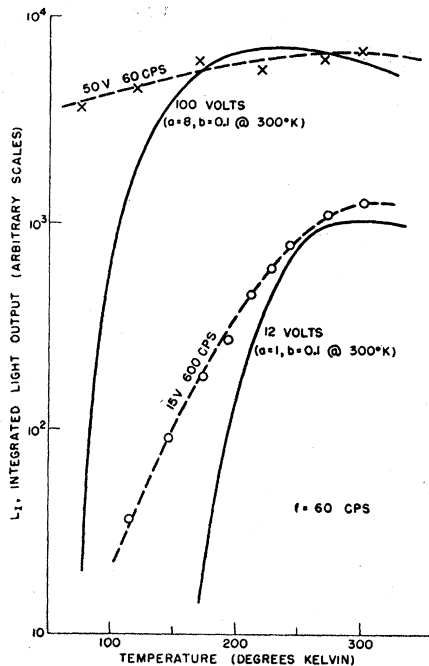


FIG. 13. Integrated light output  $L_I$  vs temperature  $T$ . Solid curves theoretical, plotted points experimental.

<sup>11</sup> W. Hoogenstraeten, *J. Electrochem. Soc.* **100**, 356 (1953).

<sup>12</sup> H. W. Leverenz, *Luminescence of Solids* (John Wiley and Sons, New York, 1950) p. 177 ff.

<sup>13</sup> R. E. Halsted and L. R. Koller, *Phys. Rev.* **93**, 349 (1954).

based upon the presence of a single trap level near 0.3 ev.

## 5. SUMMARY AND DISCUSSION

Equation (1) describes the field-controlled thermal release, from trapping states at a single level, of electrons which are regarded as subsequently contributing to luminescence processes. The three exponential factors describe the release rate as a function of time, temperature, applied voltage, and frequency; the release rate is considered proportional to the instantaneous light emission which is detected as the primary peak in the electroluminescence wave form. Equation (1) is fitted to an experimental wave form observed under certain conditions of temperature, voltage, and frequency, and the parameters  $a$  and  $b$  evaluated. From these, approximate values of trap depth and dimension can be inferred. Next, variation of parameters  $a$  and  $b$  leads to theoretical dependences of wave form on temperature, voltage, and frequency of excitation; integration yields dependences of integrated light output on the same variables.

Experimental data support the simple theory represented by Eq. (1) in the following respects. First, the left-hand exponential factor accounts for the facts that very large zero-field emission levels are observed at room temperature, and decrease sharply with decrease in temperature; this observation is made at the point in the wave form corresponding to  $t=0$ ,  $V=0$ , when the time-dependent exponential factors on the right take on the value unity. Second, these time-dependent factors determine the wave form, and the initial fit to the experimental trace can be made close. The corresponding trap depth is not only equivalent to glow-curve results for the ZnS phosphors used, but is at a level (0.3 ev) often associated with the zinc sulfide lattice, quite independent of activator or method of preparation. Third, the shifts of the experimental peaks in phase (time or voltage) with variation in peak voltage, frequency, and temperature, are in the sense and of about the magnitude predicted by these two exponential factors—with the single exception of the temperature shift in the neighborhood of  $-200^\circ\text{C}$ , for which an explanation is given. Peak heights with variation in frequency are in accord with the theory. Theory and experimental confirmation are, up to this point, independent of the ionization process, since the factor  $N_0$  has not been considered. This factor will, however, affect the theoretical integrated light output if it is a function of voltage, frequency or temperature. Apparently  $N_0$  is a function of the first two variables; however, this dependence is determined experimentally and divided out. When this is done, the theory is in agreement with the experimental dependence of  $L_I$  on frequency, temperature, and voltage to the following

extent. As regards frequency, at very low voltages good agreement is obtained since, in the absence of depletion,  $N_0$  is expected to be frequency-independent; at high voltages  $N_0 \propto f^{\frac{1}{2}}$  experimentally and is related to the observed slope at high frequencies. The usual linear increase at low frequencies, followed by a weaker dependence at higher frequencies, is predicted and observed. The predicted temperature dependence of  $L_I$  is in accord with present data and with observations of other workers, except for certain phosphors at very low temperatures where an additional mechanism has been called upon in any case. The predicted voltage dependence of Eq. (1) is of the form  $\exp(-C/E)$ ;  $N_0$  follows experimentally the same form. The product of these, integrated light output  $L_I$ , is observed to show the same voltage dependence. This well-known function has been often associated<sup>1-5</sup> with the ionization process in electroluminescence.

TABLE I. Characteristics of electroluminescence of a number of phosphors of the zinc sulfide type.

ZnS:Ag		blue	primary+small secondary
ZnS:Cu, Ag		blue	primary+small secondary
ZnS:Cu, Al		green	primary+small secondary
ZnS:Cu, Mn		yellow	primary, no secondary
Zn(S, Se):Cu		green	primary+small secondary
(Zn, Cd)S:Ag	60:40	green	primary, secondary equal
(Zn, Cd)S:Ag	50:50	yellow	primary, secondary equal
(Zn, Cd)S:Ag	15:85	red	primary, secondary equal
ZnS:Cu, Ag		blue green	phosphorescent, deep traps, in-phase electroluminescence only
(Zn, Cd)S:Cu	88:12	yellow	phosphorescent, deep traps, in-phase electroluminescence only
(Zn, Cd)S:Cu	76:24	orange	phosphorescent, deep traps, in-phase electroluminescence only

This theory of the electroluminescence wave form primarily involves electron trapping, release, and light emission processes, following the ionization of activator centers at some point in the cycle. The theory is completely independent of the mechanisms of ionization of the centers. The theory of the primary peak as given by Eq. (1) is the major consideration of this paper. Correlation to experiment, to the extent shown above, has been obtained without consideration of the secondary peak, or of the color content of light emission during either peak.

This behavior is characteristic of many, and perhaps all, zinc-sulfide-like materials. The primary peak shape described by Eq. (1) is present in the electroluminescent wave form of a number of nonphosphorescent zinc-sulfide-containing phosphors (Table I). In the zinc sulfides, the secondary peak is small, and practically nonexistent in the manganese-activated type. In the zinc cadmium sulfides, the primary peak is of typical

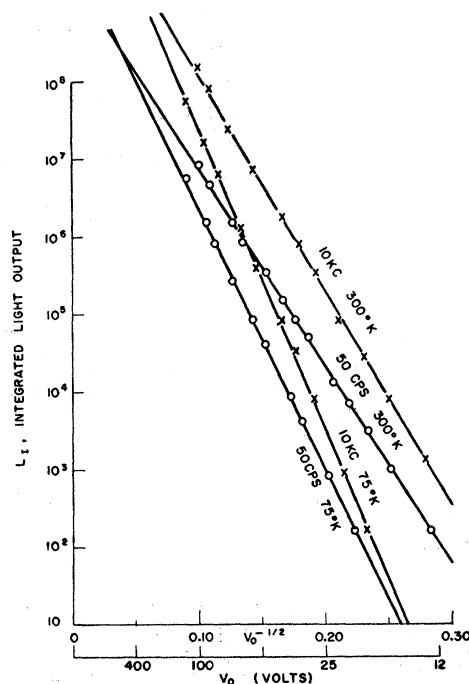


FIG. 14. Integrated light output  $L_I$  vs peak voltage  $V_0^{-\frac{1}{2}}$  with variation in frequency and temperature.

shape and the secondary peak is large, the primary and secondary peaks being about equal in area. Finally, in phosphorescent materials containing deep traps associated with the copper activator, only in-phase electroluminescence is observed; presumably the traps are too deep for field release at room temperature and normal voltages except at the voltage maxima. The

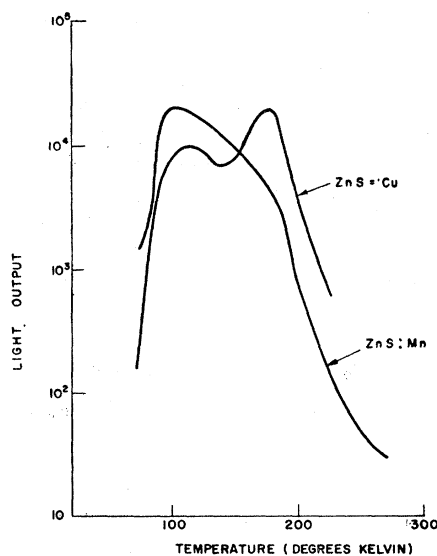


FIG. 15. Thermal glow curves for ZnS electroluminescent phosphors emitting in the blue-green and yellow.



typical primary peak shape is apparently associated with the trapping level near 0.3 eV characteristic of the zinc-sulfide-like crystal lattice. Where this 0.3-eV trap is the deepest trapping level present, no in-phase light emission at low frequencies is observed, since recombination occurs by field-controlled thermal release earlier in the voltage cycle.

#### ACKNOWLEDGMENTS

It is a pleasure to acknowledge the help of many of my colleagues and to thank particularly R. E. Halsted, P. D. Johnson, W. W. Piper, V. L. Stout, F. E. Williams, and J. R. Young for valuable discussion, and P. E. Pashler for continued encouragement. H. C. Froelich kindly supplied the electroluminescent phosphors.

## Thermoelectric Power, Electrical Resistance, and Crystalline Structure of Carbons\*†

E. E. LOEBNER‡

*Department of Physics, University of Buffalo, Buffalo, New York*

(Received April 25, 1955)

The thermoelectric power  $\Theta$  and the electric resistance  $R$  of soft and hard carbons were investigated as functions of heat-treatment temperature  $T_{ht}$  from 1000°C to 3100°C at three ambient temperatures  $T$  equal to 90°K, 305°K, and 573°K. The crystalline structure was studied by means of x-ray powder diffraction technique. For a given  $T$ , with increase of  $T_{ht}$  the thermoelectric power of soft carbons goes through a flat minimum at  $T_{ht} \sim 1400^\circ\text{C}$ , increases quite fast to a maximum at about 2100°C, and subsequently drops down again and continues to do so up to the highest  $T_{ht}$ . The electric resistance is only very slowly decreasing (plateau) up to  $T_{ht} \sim 2000^\circ\text{C}$ , with a subsequent rapid decrease up to the highest  $T_{ht}$  investigated. The positions of the maximum in  $\Theta$  and of the corresponding knee in resistance

(end of plateau) shifts to higher heat treatments with decrease of ambient temperature  $T$ . The thermoelectric power is proportional to temperature  $T$  in the range of heat treatments below the  $T_{ht}$  corresponding to the maximum in  $\Theta$ . The observed dependence of  $\Theta$  and of  $R$  on  $T_{ht}$  and  $T$  are in good agreement with Mrozowski's energy band scheme for carbons and graphites. A hard carbon prepared from phenol-benzaldehyde resin shows a two-stage graphitization with  $\frac{1}{3}$  of the crystalline mass beginning to graphitize at  $T_{ht} \sim 2200^\circ\text{C}$  and the remainder only above  $T_{ht} = 2800^\circ\text{C}$ . Correspondingly the resistance curves show two plateaus ending one at  $T_{ht} \sim 2200^\circ\text{C}$  and the other at  $T_{ht} \sim 2800^\circ\text{C}$ . The dependence of  $\Theta$  on  $T_{ht}$  is somewhat similar to that found in soft carbons.

### I. INTRODUCTION

ELECTRICAL properties of carbons have been investigated extensively during the past sixty years. In 1916 La Rosa<sup>1</sup> reviewed the earliest work on the thermoelectric power of carbon and noted large differences in the values previously published by other investigators. In the same paper he also reported results of his measurements of the thermoelectric power for a purified<sup>2</sup> carbon at temperatures between 308°K and 823°K. He found that the thermoelectric power, relative to a platinum standard, had a positive sign and increased linearly with temperature. Knowing that carbon has a negative coefficient of resistance, which is characteristic of "variable conductors" (semiconductors), the linear increase, which is characteristic of metals, seemed anomalous to La Rosa. Comparing his results with those of his predecessors, La Rosa attributed the large disagreements in magnitude and temperature dependence (after normalization to the

same standard) to possible experimental difficulties or the presence of impurities in the samples of the other investigators, rather than to differences in the manufacturing processes (arc lamp carbon rods, carbon filaments, etc.).

Gottstein,<sup>3</sup> who checked the validity of thermodynamic relationships between different thermoelectric effects for a number of semiconductors, reported the value of the thermoelectric power of natural graphite (unknown purity) to be  $+9.76 \mu\text{V}/^\circ\text{K}$  with respect to copper when measured directly and  $+9.97 \mu\text{V}/^\circ\text{K}$  when calculated from the measured values of the Peltier coefficient.

In the period between the two world wars, little was published on the thermoelectric behavior of carbons and graphite. Pirani and Fehse<sup>4</sup> reported the thermoelectric power of a highly graphitized ("metallized") incandescent lamp filament to be  $+2.5 \mu\text{V}/^\circ\text{K}$  with respect to platinum. Some measurements were made also by Fukuda and Saito<sup>5</sup> on carbon films formed by thermal decomposition of aliphatic hydrocarbons in vacuo at about 1100°C. They reported the thermoelectric power as negative with respect to copper (the authors also claim a negative sign for graphite with

\* Supported by the Office of Naval Research. Reproduction in whole or in part is permitted for any purpose of the United States Government.

† This paper is based in part on part of a thesis submitted in partial fulfillment of the requirements for the degree of Doctor of Philosophy at the University of Buffalo.

‡ Present address: RCA Laboratories, Princeton, New Jersey.

<sup>1</sup> M. La Rosa, *Nuovo cimento* **12**, 284 (1916).

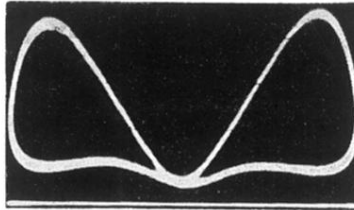
<sup>2</sup> M. La Rosa purified a commercial carbon rod by keeping it for nine hours at about 800°C in a stream of chlorine.

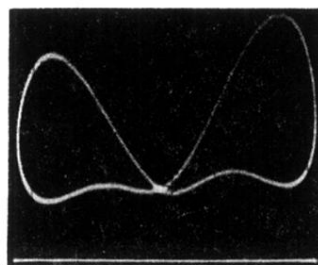
<sup>3</sup> G. Gottstein, *Ann. Physik* **43**, 1079 (1914).

<sup>4</sup> M. Pirani and W. Fehse, *Z. Electrochem.* **29**, 168 (1929).

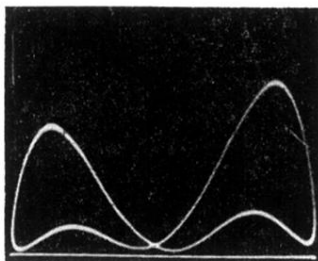
<sup>5</sup> M. Fukuda and Y. Saito, *Electrotech. J. (Japan)* **2**, 129 (1938).

FIG. 1. Experimental light-output wave form; 60 cps, 50 volts rms, room temperature. Light increasing upward, instantaneous voltage zero at center, maximum at left and right.





-20°C



-196°C

FIG. 3. Oscilloscope traces illustrating the temperature dependence of light output at  $V=0$ .  $F=60$  cps;  $V=50$  volts rms.

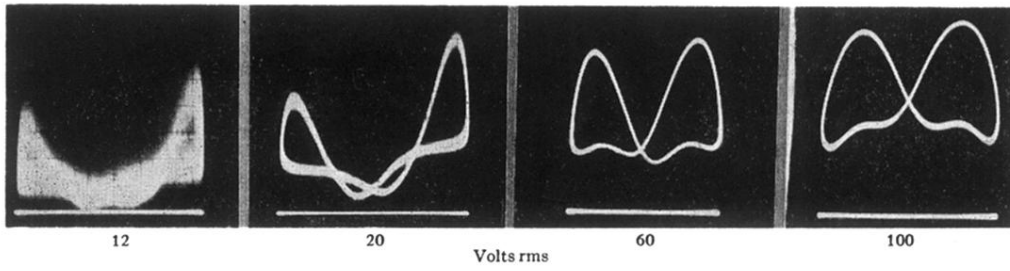


FIG. 5. Experimental wave forms showing the peak shift toward earlier times with increase in peak voltage  $V_0$ .  $F = 60$  cps;  $T = +30^\circ\text{C}$ .

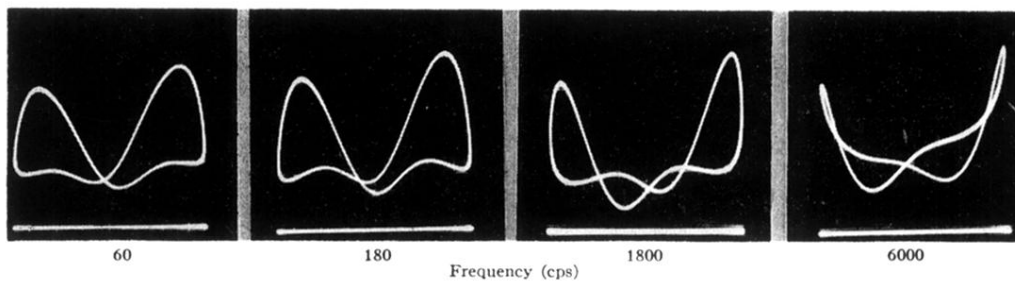


FIG. 7. Experimental wave forms with variation in frequency.  $T = 30^{\circ}\text{C}$ ,  $V = 50$  volts rms.

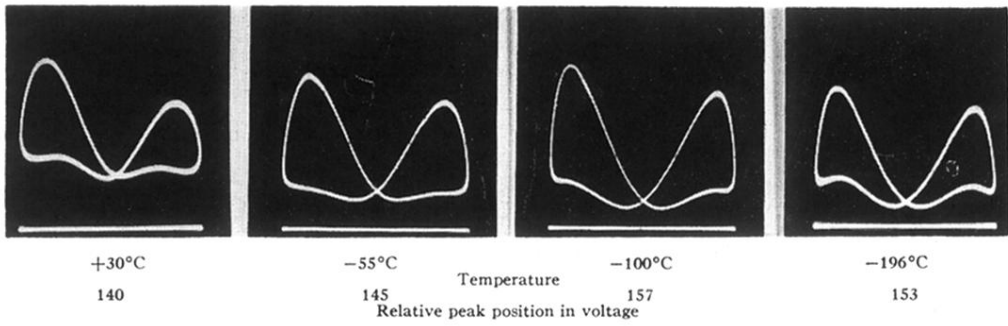


FIG. 9. Experimental wave forms with variation in temperature.  $f = 60$  cps;  $V = 50$  volts rms.